

American Mineralogist

Supporting Information for

Single-crystal Elasticity of Humite-Group Minerals by Brillouin Scattering

QINGCHUN ZHANG¹, XINYUE ZHANG¹, LUO LI¹, ZHU MAO^{1,2,3,*}, XIANG WU⁴

¹Deep Space Exploration Laboratory / School of Earth and Space Sciences, University of Science and Technology of China, Hefei 230026, China

²CAS Center for Excellence in Comparative Planetology, University of Science and Technology of China, Hefei, Anhui 230026, China

³Frontiers Science Center for Planetary Exploration and Emerging Technologies, University of Science and Technology of China, Hefei, Anhui 230026, China

⁴State Key Laboratory of Geological Processes and Mineral Resources, China University of Geosciences, Wuhan 430074, China

*Corresponding authors: Zhu Mao (zhumao@ustc.edu.cn)

Contents of this file

Figures S1 to S3

Tables S1 to S10

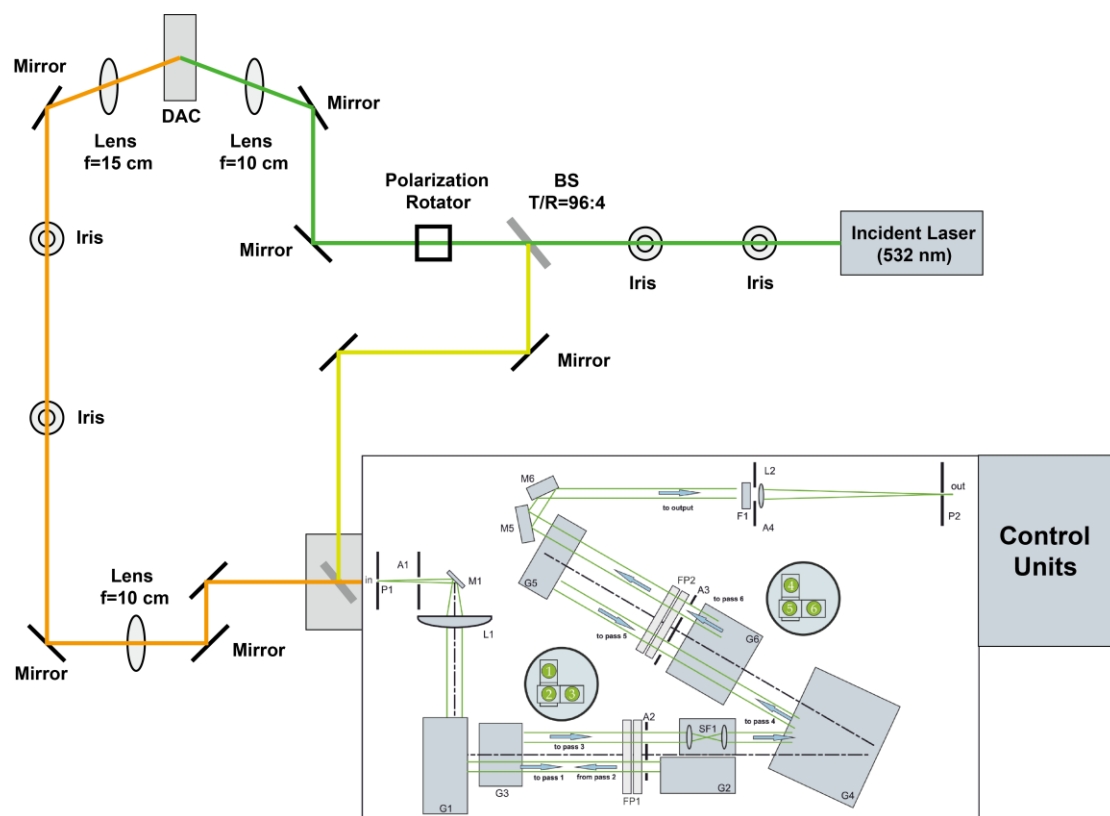


Figure S1. Schematic diagram of the Brillouin scattering setup.

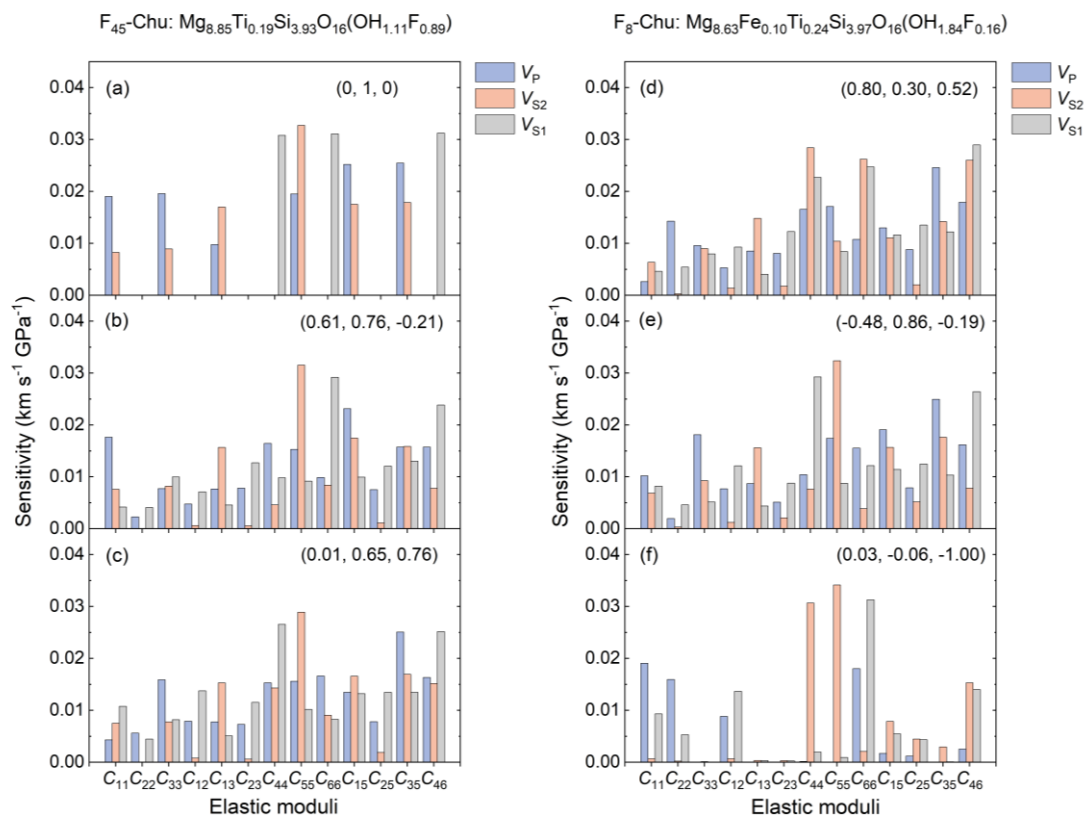


Figure S2. Sensitivity of each C_{ij} to the measured sound velocities in each sample platelet. (a)-(c): F₄₅-clinohumite; (d-f): F₈-clinohumite. The orientations of the crystal platelets are given in parentheses.

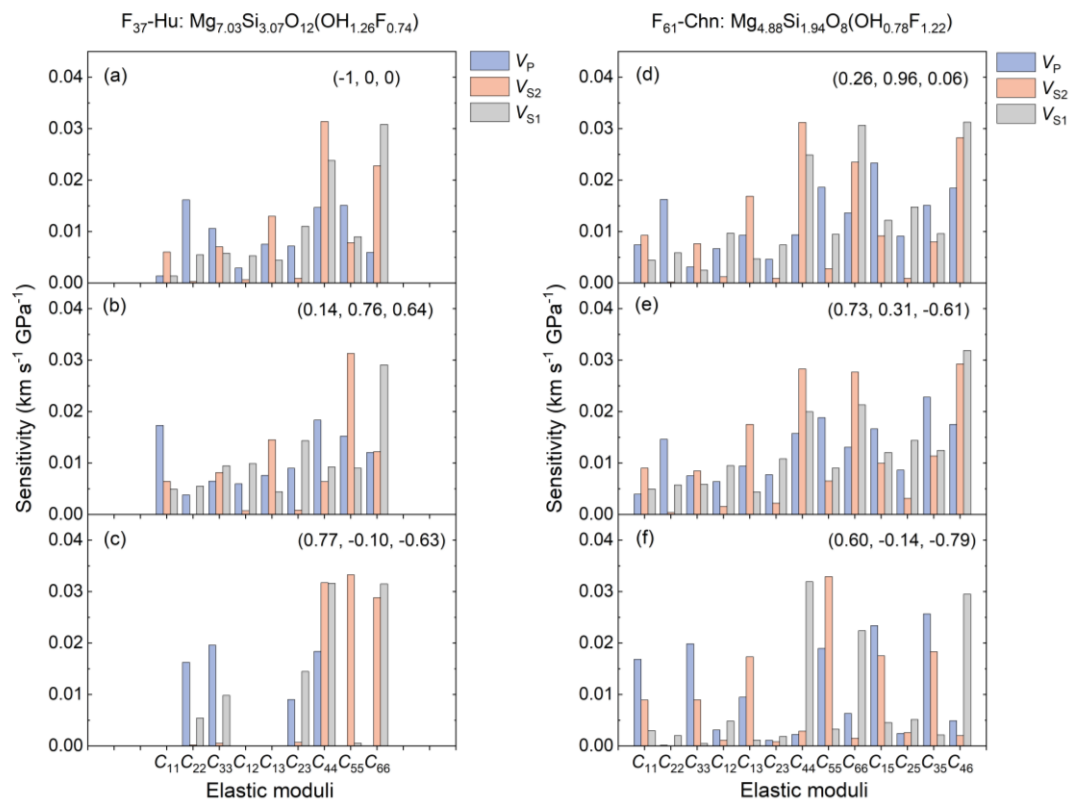


Figure S3. Sensitivity of each C_{ij} s to the measured sound velocities in each sample platelet. (a)-(c): F₃₇-humite; (d-f): F₆₁-chondrodite. The orientations of the crystal platelets are given in parentheses.

	V_S (km/s)	V_{S_error}	V_P (km/s)	V_{P_error}
This study	3.71	0.13%	6.07	0.3%
Polian et al. (2002)	3.74	N/A	5.95	N/A
Error	-0.8%		1.9%	

Table S1. Acoustic velocities comparison of glass as a standard material.

(h, k, l)	Degree (°)	V _P (km/s)	Degree (°)	V _{S2} (km/s)	Degree (°)	V _{S1} (km/s)
(0, 1, 0)	0	8.11832	0		0	4.70121
	10	8.19984	10		10	4.63952
	20	8.31806	20		20	4.56301
	30	8.41905	30		30	4.57113
	40	8.42148	40		40	4.59394
	50	8.38338	50		50	4.65029
	60	8.27149	60		60	4.7062
	70	8.16349	70		70	4.72841
	80	8.07795	80		80	4.73983
	90	8.00836	90		90	4.70568
	100	7.93513	100		100	4.60534
	110	7.89222	110		110	4.53611
	120	7.88927	120		120	4.50597
	130	7.82313	130		130	4.53737
	140	7.84149	140		140	4.6188
	150	7.84122	150		150	4.67864
	160	7.87261	160		160	4.73021
	170	8.01274	170		170	4.73141
	180	8.1318	180		180	4.68144
(0.61, 0.76, -0.21)	0	8.60693	0	5.30204	0	4.78303
	10	8.55647	10	5.38299	10	4.66698
	20	8.55671	20	5.3785	20	4.65092
	30	8.53839	30	5.35913	30	4.63876
	40	8.51201	40	5.28505	40	4.61628
	50	8.49859	50	5.1477	50	4.6337
	60	8.42104	60	5.05583	60	4.65742
	70	8.33465	70	4.96147	70	4.68552
	80	8.28199	80	4.9097	80	
	90	8.24242	90	5.09848	90	4.81841
	100	8.24646	100	5.19115	100	4.77935
	110	8.29682	110	5.23906	110	4.79259
	120	8.36023	120	5.27023	120	4.77432
	130	8.48298	130	5.26315	130	4.76006
	140	8.60021	140	5.23554	140	4.75118
	150	8.6441	150	5.26857	150	4.75599
	160	8.65383	160	5.27567	160	4.79326
	170	8.64265	170	5.27002	170	4.80337
	180	8.60183	180	5.28598	180	4.77432
	0	7.92217	0	4.8828	0	
	10	7.95681	10	4.88524	10	
	20	8.08959	20	5.077	20	4.79375
	30	8.23164	30	5.21655	30	4.7745
	40	8.46706	40	5.35984	40	4.778

(-0.17, 0.46, -0.87)	50	8.75319	50	5.43296	50	4.79718
	60	9.00307	60	5.45742	60	4.82354
	70	9.27053	70	5.38791	70	4.83107
	80	9.41881	80	5.31425	80	4.85203
	90	9.54311	90		90	4.92361
	100	9.51529	100		100	4.95472
	110	9.36236	110	5.22471	110	4.95776
	120	9.09703	120	5.27229	120	4.89341
	130	8.87626	130	5.34577	130	4.89511
	140	8.54878	140	5.35965	140	
	150	8.33443	150	5.30129	150	
	160	8.18119	160	5.19944	160	
	170	8.09757	170	5.04396	170	
	180	8.11631	180	4.96423	180	

Table S2. Acoustic velocities as a function of laboratory angle for the three F₄₅-clinohumite platelets. The uncertainty of the measured velocities is <0.7%.

(h, k, l)	Degree (°)	V _P (km/s)	Degree (°)	V _{S2} (km/s)	Degree (°)	V _{S1} (km/s)
(0.03, -0.06, -1)	0	9.64092	0	4.97344	0	
	10	9.49926	10	4.99533	10	
	20	9.21587	20	5.12875	20	
	30	8.93225	30	5.25484	30	
	40	8.59255	40	5.30845	40	
	50	8.38254	50	5.2812	50	
	60	8.19454	60	5.1568	60	
	70	8.08604	70	5.06266	70	
	80	8.08548	80	4.93233	80	
	90	8.13736	90	4.96539	90	
	100	8.179	100	5.11159	100	
	110	8.29282	110	5.23777	110	
	120	8.4344	120	5.33356	120	
	130	8.72969	130	5.34909	130	
	140	9.05471	140	5.27288	140	
	150	9.38736	150	5.13455	150	
	160	9.60929	160	5.02684	160	
	170	9.70922	170	4.92168	170	
	180	9.69063	180	4.98288	180	
(0.80, 0.30, 0.52)	0	8.36438	0	5.24706	0	
	10	8.13333	10	5.1696	10	
	20	8.04029	20	5.02028	20	
	30	8.03029	30	4.90231	30	
	40	8.0627	40	4.8865	40	
	50	8.09513	50	4.99288	50	
	60	8.19605	60	5.148	60	4.79325
	70	8.32732	70	5.29423	70	4.70143
	80	8.54048	80	5.38584	80	4.72589
	90	8.84863	90	5.35542	90	4.72019
	100	9.09623	100	5.24663	100	4.72195
	110	9.33589	110	5.14387	110	4.78253
	120	9.43965	120	5.00883	120	4.79528
	130	9.4521	130		130	4.84736
	140	9.37536	140	4.89768	140	
	150	9.18693	150	5.01242	150	
	160	8.91108	160	5.12763	160	
	170	8.56713	170	5.22439	170	
	180	8.32862	180	5.21977	180	
	0	8.38156	0		0	4.5208
	10	8.32374	10		10	4.56921
	20	8.26985	20		20	4.61074
	30	8.20293	30		30	4.65447
	40	8.12308	40		40	4.74339

(-0.48, 0.86, -0.19)	50	8.03981	50	50	4.71644
	60	7.98293	60	60	4.66377
	70	7.93221	70	70	4.57494
	80	7.85854	80	80	4.50708
	90	7.83253	90	90	4.49213
	100	7.82928	100	100	4.56178
	110	7.8122	110	110	4.62213
	120	7.85009	120	120	4.6722
	130	7.92099	130	130	4.69799
	140	8.03912	140	140	4.68949
	150	8.16659	150	150	4.64588
	160	8.2769	160	160	4.56616
	170	8.34115	170	170	4.51766
	180	8.36438	180	180	4.50568

Table S3. Acoustic velocities as a function of laboratory angle for the three F₈-clinohumite platelets. The uncertainty of the measured velocities is <0.7%.

(h, k, l)	Degree (°)	V _P (km/s)	Degree (°)	V _{S2} (km/s)	Degree (°)	V _{S1} (km/s)
(0.14, 0.76, 0.64)	0	9.04456	0	4.98321	0	4.85398
	10	8.76399	10	5.12863	10	
	20	8.47486	20	5.21611	20	
	30	8.17191	30	5.17067	30	
	40	8.00246	40	5.05337	40	
	50	7.93011	50	4.9038	50	
	60	7.8922	60	4.80482	60	
	70	7.89026	70	4.81357	70	
	80	7.97599	80	4.94576	80	
	90	8.11161	90	5.11318	90	
	100	8.30499	100	5.18671	100	
	110	8.60279	110	5.23163	110	
	120	8.98573	120	5.18054	120	
	130	9.21078	130	5.04137	130	
	140	9.48601	140	4.8642	140	
	150	9.56945	150	4.83944	150	
	160	9.56402	160	4.85511	160	
	170	9.38563	170	4.95019	170	
	180	9.12982	180	5.05035	180	
(-1, 0, 0)	0	8.03531	0	4.87593	0	4.77081
	10	7.99065	10	4.841	10	
	20	7.9984	20	4.9531	20	
	30	8.09728	30	5.09737	30	
	40	8.3673	40	5.27423	40	
	50	8.64567	50	5.28389	50	
	60	8.94083	60	5.23289	60	
	70	9.20117	70	5.04488	70	
	80	9.41568	80		80	
	90	9.47687	90		90	
	100	9.51677	100		100	
	110	9.43577	110	4.99133	110	
	120	9.17746	120	5.17703	120	
	130	8.86342	130	5.2629	130	
	140	8.5723	140	5.29885	140	
	150	8.30557	150	5.24659	150	
	160	8.11127	160	5.1471	160	
	170	8.05339	170	4.98282	170	
	180	8.09548	180		180	
	0	8.38761	0		0	4.72451
	10	8.31726	10	5.1832	10	4.71652
	20	8.27899	20	5.20481	20	4.70218
	30	8.19513	30	5.18803	30	4.6929

(0.77, -0.10, -0.63)	40	8.20241	40	5.18348	40	4.67142
	50	8.15606	50	5.13091	50	4.65537
	60	8.22376	60	5.08673	60	4.64548
	70	8.18151	70	4.98282	70	4.59237
	80	8.23169	80	4.98117	80	4.6506
	90	8.24166	90	4.9109	90	4.62982
	100	8.27494	100	4.98605	100	4.63255
	110	8.23901	110	5.05071	110	4.65299
	120	8.22211	120	5.11363	120	4.67088
	130	8.32042	130	5.16936	130	4.70451
	140	8.38491	140	5.26836	140	4.7383
	150	8.39985	150	5.29411	150	4.74429
	160	8.39482	160	5.28645	160	4.7615
	170	8.43533	170		170	4.81339
	180	8.47691	180		180	4.79723

Table S4. Acoustic velocities as a function of laboratory angle for the three F₃₇-humite platelets. The uncertainty of the measured velocities is <0.7%.

(h, k, l)	Degree (°)	V _P (km/s)	Degree (°)	V _{S2} (km/s)	Degree (°)	V _{S1} (km/s)
(0.26, 0.96, 0.06)	0	7.96986	0		0	4.7769
	10	7.88425	10		10	4.76256
	20	7.868	20		20	4.68045
	30	7.90913	30		30	4.569
	40	7.94848	40		40	4.46269
	50	7.97386	50		50	4.44038
	60	8.00484	60		60	4.48117
	70	7.92525	70		70	4.58432
	80	7.90711	80		80	4.69169
	90	7.92035	90		90	4.76214
	100	7.95811	100		100	4.75917
	110	8.03071	110		110	4.66114
	120	8.14309	120		120	4.56881
	130	8.1747	130		130	4.45841
	140	8.21003	140		140	4.44083
	150	8.17519	150		150	4.47106
	160	8.1215	160		160	4.58017
	170	8.04897	170		170	4.7116
	180	7.98314	180		180	4.77798
(0.03, -0.06, -1)	0	8.19644	0	5.13472	0	
	10	8.36878	10	5.23471	10	
	20	8.64924	20	5.24964	20	
	30	8.92283	30	5.15765	30	
	40	9.15384	40	5.05651	40	
	50	9.41565	50	4.93105	50	
	60	9.49976	60	4.84562	60	
	70	9.50476	70	4.86425	70	
	80	9.35771	80	4.98281	80	
	90	9.13947	90	5.12051	90	
	100	8.86636	100	5.24192	100	
	110	8.59701	110	5.3098	110	
	120	8.36716	120	5.27801	120	
	130	8.23507	130	5.15765	130	
	140	8.16124	140	5.00003	140	
	150	8.13879	150	4.88538	150	
	160	8.14348	160	4.90922	160	
	170	8.19433	170	5.04935	170	
	180	8.26006	180	5.16106	180	
	0	8.20982	0	4.91918	0	
	10	8.25537	10	4.91259	10	
	20	8.26083	20	5.02794	20	
	30	8.35603	30	5.16139	30	

(0.73, 0.31, -0.61)	40	8.48824	40	5.23555	40
	50	8.63398	50	5.1806	50
	60	8.88752	60	5.1476	60
	70	9.09558	70	5.03074	70
	80	9.27434	80	4.97464	80
	90	9.38501	90	4.92276	90
	100	9.33396	100	4.94181	100
	110	9.20967	110	5.02016	110
	120	8.96876	120	5.14471	120
	130	8.74547	130	5.22155	130
	140	8.52227	140	5.26452	140
	150	8.34919	150	5.19856	150
	160	8.218	160	5.10867	160
	170	8.16709	170	4.97683	170
	180	8.18659	180	4.91124	180

Table S5. Acoustic velocities as a function of laboratory angle for the three F₆₁-chondrodite platelets. The uncertainty of the measured velocities is <0.7%.

	C_{11}	C_{22}	C_{33}	C_{44}	C_{55}	C_{66}	C_{12}	C_{13}	C_{23}	C_{15}	C_{25}	C_{35}	C_{46}
C_{11}	1.00	-0.09	-0.14	0.11	-0.21	-0.22	0.04	0.06	-0.04	0.01	0.04	0.07	-0.04
C_{22}		1.00	-0.06	-0.33	0.07	-0.17	0.16	-0.18	0.12	-0.05	-0.07	0.00	-0.06
C_{33}			1.00	-0.36	-0.21	0.11	-0.09	0.32	0.26	0.05	0.04	-0.03	0.04
C_{44}				1.00	-0.16	-0.25	0.06	-0.01	-0.42	0.02	0.00	0.06	0.00
C_{55}					1.00	-0.06	0.01	-0.10	0.07	-0.11	0.09	-0.01	0.02
C_{66}						1.00	-0.11	0.05	0.09	0.01	-0.06	-0.06	0.03
C_{12}							1.00	0.00	-0.31	0.04	-0.18	0.02	-0.08
C_{13}								1.00	0.05	0.12	0.07	-0.02	0.03
C_{23}									1.00	0.02	0.08	0.02	0.00
C_{15}										1.00	0.14	0.09	-0.23
C_{25}											1.00	0.14	-0.13
C_{35}												1.00	-0.23
C_{46}													1.00

Table S6. Correlation matrices obtained from the inversion of acoustic velocities of the three F₄₅-clinohumite platelets.

	C_{11}	C_{22}	C_{33}	C_{44}	C_{55}	C_{66}	C_{12}	C_{13}	C_{23}	C_{15}	C_{25}	C_{35}	C_{46}
C_{11}	1.00	-0.01	0.09	-0.02	-0.15	-0.39	-0.05	0.36	-0.18	0.35	-0.19	0.21	-0.13
C_{22}		1.00	0.06	-0.15	0.01	-0.19	-0.09	0.05	-0.11	0.11	-0.21	0.08	0.02
C_{33}			1.00	-0.30	-0.24	0.01	-0.20	0.42	-0.20	0.35	-0.26	0.47	-0.13
C_{44}				1.00	-0.19	-0.06	0.04	-0.09	-0.09	-0.22	-0.02	-0.12	0.25
C_{55}					1.00	-0.03	0.05	-0.10	0.07	0.03	0.11	0.13	-0.05
C_{66}						1.00	-0.18	-0.05	-0.06	-0.12	-0.13	-0.07	0.34
C_{12}							1.00	-0.24	0.18	-0.21	0.51	-0.16	-0.20
C_{13}								1.00	-0.38	0.53	-0.40	0.49	-0.03
C_{23}									1.00	-0.24	0.64	-0.30	-0.12
C_{15}										1.00	-0.23	0.30	-0.33
C_{25}											1.00	-0.27	-0.29
C_{35}												1.00	-0.15
C_{46}													1.00

Table S7. Correlation matrices obtained from the inversion of acoustic velocities of the three F₈-clinohumite platelets.

	C_{11}	C_{22}	C_{33}	C_{44}	C_{55}	C_{66}	C_{12}	C_{13}	C_{23}
C_{11}	1.00	-0.09	0.13	-0.04	0.02	-0.08	0.05	-0.27	-0.19
C_{22}		1.00	0.09	0.13	-0.38	-0.09	-0.02	0.05	0.07
C_{33}			1.00	-0.10	-0.01	0.12	-0.06	-0.15	0.12
C_{44}				1.00	0.01	-0.12	-0.27	0.01	-0.02
C_{55}					1.00	0.25	-0.18	-0.03	-0.01
C_{66}						1.00	-0.35	-0.28	0.06
C_{12}							1.00	0.01	-0.21
C_{13}								1.00	-0.19
C_{23}									1.00

Table S8. Correlation matrices obtained from the inversion of acoustic velocities of the three F₃₇-humite platelets.

	C_{11}	C_{22}	C_{33}	C_{44}	C_{55}	C_{66}	C_{12}	C_{13}	C_{23}	C_{15}	C_{25}	C_{35}	C_{46}
C_{11}	1.00	0.29	-0.14	-0.16	-0.44	-0.48	-0.38	0.28	-0.34	-0.01	0.41	-0.19	0.34
C_{22}		1.00	-0.01	-0.46	-0.16	-0.52	-0.56	0.14	-0.50	-0.03	0.63	-0.18	0.50
C_{33}			1.00	-0.14	-0.28	0.08	-0.02	0.10	0.06	-0.08	-0.01	-0.06	0.03
C_{44}				1.00	0.06	0.23	0.44	-0.12	0.31	0.24	-0.44	0.06	-0.73
C_{55}					1.00	0.20	0.22	-0.32	0.19	-0.07	-0.23	-0.02	-0.16
C_{66}						1.00	0.48	-0.19	0.48	-0.18	-0.55	0.24	-0.69
C_{12}							1.00	-0.24	0.56	0.07	-0.88	0.18	-0.53
C_{13}								1.00	-0.20	-0.12	0.26	-0.31	0.16
C_{23}									1.00	0.00	-0.84	0.17	-0.44
C_{15}										1.00	-0.04	-0.16	-0.13
C_{25}											1.00	-0.18	0.56
C_{35}												1.00	-0.21
C_{46}													1.00

Table S9. Correlation matrices obtained from inversion of acoustic velocities of the three F₆₁-chondrodite platelets.

Mineral	$C_{\text{H}_2\text{O}}$	ρ (g/cm ³)	K_{S0} (GPa)	G_0 (GPa)	V_{P} (km/s)	V_{S} (km/s)
Opx ¹	0	3.329(4)	107.8(7)	77.1(6)	7.96(4)	4.81(2)
Cpx ²	0	3.327(1)	116.0(6)	72.6(4)	8.08(2)	4.71(1)
Ol ³	0	3.343(3)	129.8(9)	77.8(5)	8.36(1)	4.82(1)
Garnet ⁴	0	3.641(3)	173.1(5)	92.5(9)	9.02(2)	5.04(1)
Wads ⁵	0	3.57(3)	170(3)	108(2)	9.38(4)	5.50(3)
Maj ⁶	0	3.629(7)	165.9(8)	92.3(4)	8.92(2)	5.04(1)
phA ⁷	11.8	2.973(2)	102.1(5)	66.7(3)	8.02(1)	4.74(1)
Fe-phA ⁸	11.7	2.976(1)	106(1)	61(1)	7.93(8)	4.53(8)
phE ⁹	11.9	2.949(1)	98.3(7)	61.0(1)	7.80(2)	4.55(1)
Fe-phE ¹⁰	12.4(4)	3.04(1)	95.9(4)	59.6(2)	7.60(2)	4.43(1)
F ₆₁ -Chon ¹¹	2.1	3.136(1)	120.4(3)	74.1(5)	8.36(2)	4.86(2)
F ₃₇ -Hu ¹²	2.4	3.207(1)	122.4(3)	78.4(2)	8.41(1)	4.94(1)
F ₈ -Chu ¹³	2.6	3.219(1)	120.5(3)	76.8(2)	8.32(1)	4.88(1)
F ₄₅ -Chu ¹⁴	1.6	3.208(1)	126.2(3)	79.7(2)	8.51(1)	4.98(1)

¹Opx: orthopyroxene (Li et al., 2022); ²Cpx: diopside (Li and Neuville, 2010); ³Ol: olivine (Mao et al., 2015); ⁴Garnet: pyrope (Wei et al., 2021); ⁵Wads: wadsleyite (Mao et al., 2015); ⁶Maj: majorited-garnet (Wei et al., 2021); ⁷phA: Fe-free phase A (Cai et al., 2021); ⁸Fe-phA: Fe-bearing phase A (Sanchez-Valle et al., 2006); ⁹phE: Fe-free E (Wang et al., 2022); ¹⁰Fe-phE: Fe-bearing phase E (Satta et al., 2019); ¹¹F₆₁-Chon: chondrodite with $X_{\text{F}}=0.61$; ¹²F₃₇-Hu: humite with $X_{\text{F}}=0.37$; ¹³F₈-Chu: clinohumite with $X_{\text{F}}=0.08$; ¹⁴F₄₅-Chu: F₄₅-clinohumite with $X_{\text{F}}=0.45$.

Table S10. Elastic parameters of humite-group minerals and major mantle minerals.

Reference

- Cai, N., Qi, X., Chen, T., Wang, S., Yu, T., Wang, Y., Inoue, T., Wang, D., and Li, B. (2021) Enhanced Visibility of Subduction Slabs by the Formation of Dense Hydrous Phase A. *Geophysical Research Letters*, 48(19), e2021GL095487.
- Li, B., and Neuville, D.R. (2010) Elasticity of diopside to 8GPa and 1073K and implications for the upper mantle. *Physics of the Earth and Planetary Interiors*, 183(3-4), 398-403.
- Li, L., Sun, N., Shi, W., Mao, Z., Yu, Y., Zhang, Y., and Lin, J.F. (2022) Elastic Anomalies Across the α - β Phase Transition in Orthopyroxene: Implication for the Metastable Wedge in the Cold Subduction Slab. *Geophysical Research Letters*, 49(16).
- Mao, Z., Fan, D., Lin, J.-F., Yang, J., Tkachev, S.N., Zhuravlev, K., and Prakapenka, V.B. (2015) Elasticity of single-crystal olivine at high pressures and temperatures. *Earth and Planetary Science Letters*, 426, 204-215.
- Polian, A., Dung, V.-T., and Richet, P. (2002) Elastic properties of α -SiO₂ up to 2300 K from Brillouin scattering measurements. *Europhysics Letters*, 57(3), 375.
- Sanchez-Valle, C., Sinogeikin, S.V., Smyth, J.R., and Bass, J.D. (2006) Single-crystal elastic properties of dense hydrous magnesium silicate phase A. *American Mineralogist*, 91(5-6), 961-964.
- Satta, N., Marquardt, H., Kurnosov, A., Buchen, J., Kawazoe, T., McCammon, C., and Ballaran, T.B. (2019) Single-crystal elasticity of iron-bearing phase E and seismic detection of water in Earth's upper mantle. *American Mineralogist*, 104(10), 1526-1529.
- Wang, B., Zhang, Y., Fu, S., Ding, X., Liang, W., Takahashi, E., Li, L., Tkachev, S.N., Prakapenka, V.B., and Lin, J.F. (2022) Single-crystal elasticity of phase E at high pressure and temperature: Implications for the low-velocity layer atop the 410-km depth. *Journal of Geophysical Research: Solid Earth*, 107(1), 147-152.
- Wei, W., Mao, Z., Sun, N., Sun, D., and Tkachev, S.N. (2021) High Pressure-Temperature Single-Crystal Elasticity of Grossular: Implications for the Low-Velocity Layer in the Bottom Transition Zone. *Geophysical Research Letters*, 48(9).